Theor Chim Acta (1994) 89: 213–226

Theoretica Chimica Acta

A quantum chemical method for the calculation of dynamic structure factors: Applications to silicon, magnesium oxide and beryllium oxide

Patrick Azavant, Albert Lichanot, Michel Rerat, Max Chaillet

Laboratoire de Chimie Structurale, Université de Pau et des Pays de l'Adour URA 474, I.F.R. – Rue Jules Ferry, F-64000 Pau, France

Received January 21, 1994/Accepted May 17, 1994

Summary. The static structure factors of periodic systems have been deduced from *ab initio* Hartree–Fock calculations. Taking into account atomic thermal motions, dynamic structure factors at 298 K were then calculated by assuming that atomic displacements are independent and atomic orbitals follow nuclear movements. Three triperiodic systems have been studied: silicon, magnesium oxide and beryllium oxide.

Key words: Hartree–Fock calculation – Density matrix – Dynamic structure factors

1 Introduction

The value of precisely determining the structure factors of a given compound is now an established fact. They are deduced from experimental observations and can be used for the construction of electron density maps, which furnish considerable information. Inversely theoretical structure factors can be obtained by Fourier transform of electron density. Agreement between experimentally and theoretically determined structure factors guarantees the quality of the wave function. Consequently, high quality wave functions can lead to the calculation of reliable values of other physical properties. The CRYSTAL program [1] relies on Hartree–Fock theory to allow the study of periodic systems [2] at 0 K temperature. To compare theoretically determined structure factors to experimental values, theoretical results are corrected for thermal motion via the Debye–Waller model and experimental values are corrected for secondary effects (absorption, polarization, etc.). The theoretical–experimental difference at 0 K or at a given temperature T is minimized using a least squares method to furnish optimal thermal motion factors. The optimization process yields results whose quality improves as the number of parameters to be optimized is reduced, i.e. the compound is simple (mono-atomic) and the structure is symmetrical (isotropic). In this case, the thermal motion factor is a specific diagonal and isotropic tensor for each atom. In fully ionic compounds, e.g. MgO [3], contributions from each ion in the expression of overall structure factor can be separated. They can be corrected by respective thermal motion tensors, since the projection of electron density per energy band can be unambiguously attributed to a given ion. For non-ionic compounds, thermal motion corrections should be obtained by using the total molecular wave function or crystalline orbital.

The present work proposes a novel method for the calculation of dynamic structure factors at an arbitrary temperature T, which can be used with any kind of *ab initio* determined wave function.

While in the usual technique, the electron density is first divided into atomic or ionic contributions and thermal motion is then applied independently to the individual species, our method does not require any a priori partition.

The thermal correction is applied to couples of atomic orbitals (μ, ν) with which are associated the elements of the density matrix $(\boldsymbol{P}_{\mu\nu})$, assuming that the latter remain unchanged at different temperatures.

Our method has been applied to three types of crystals presenting a variety of structure and binding type, silicon, magnesium oxide and beryllium oxide.

2 Method of calculating structure factors

Static structure factor

There exist different types of multi-photon processes when an electromagnetic wave interacts with an electron cloud. In two-photon, high-energy elastic interaction processes (Thomson scattering) the ratio of scattered wave/incident wave amplitudes, called the scattering factor, is written as

$$f(\boldsymbol{s}) = \int \rho(\boldsymbol{r}) \mathrm{e}^{-\mathrm{i}\boldsymbol{s}\cdot\boldsymbol{r}} \mathrm{d}^3 r, \tag{1}$$

where $\boldsymbol{r}$ is the electron position, $\rho(\boldsymbol{r})$ is the electron density and $\boldsymbol{s}$ is the scattering vector.

This corresponds to the mean value (first order perturbation) of the Hamiltonian of two-photon interaction obtained in the Coulomb gauge [4, 5]. $f(\boldsymbol{s})$ is thus the Fourier transform of $\rho(\boldsymbol{r})$.

In the case of periodic systems, the scattering factor (1) is null, except for the scattering vectors $\boldsymbol{s}$ that satisfy Bragg's law. When expressed on the basis of a crystal cell, it is called the structure factor and is noted $F_0(\boldsymbol{s})$. In this work, the wave function used results from a linear combination of atomic orbitals (LCAO) Hartree–Fock *ab initio* calculation [2] conducted with a program that takes the triperiodicity of the system into account (CRYSTAL [1]).

In this case, the electron density is expressed as

$$\rho(\boldsymbol{r}) = \sum_{\mu,\nu,\boldsymbol{g}} \boldsymbol{P}^{\boldsymbol{g}}_{\mu\nu}\, \chi^{\boldsymbol{0}}_{\mu}(A, \boldsymbol{r})\, \chi^{\boldsymbol{g}*}_{\nu}(B, \boldsymbol{r}), \tag{2}$$

where $\chi^{\boldsymbol{0}}_{\mu}(A, \boldsymbol{r})$ is the μth AO on atom $A(\boldsymbol{r}_A)$ in the reference zero cell, $\chi^{\boldsymbol{g}}_{\nu}(B, \boldsymbol{r})$ is the νth AO on atom $B(\boldsymbol{r}_B)$ in the crystal cell associated with the translation vector $\boldsymbol{g}$, and $\boldsymbol{P}^{\boldsymbol{g}}_{\mu\nu}$ is the corresponding element of the density matrix.

In general, each atomic orbital is developed as a linear combination of Gaussian type functions (GTFs). In the following, for simplicity and without loss of generality, we shall assume that there is only one GTF per AO.

From expressions (1) and (2), the static structure factor $F_0(\boldsymbol{s})$ can be written as follows:

$$F_0(\boldsymbol{s}) = \sum_{\mu,\nu,\boldsymbol{g}} \boldsymbol{P}^{\boldsymbol{g}}_{\mu\nu} I_{0_{\mu\nu}}(s_x) I_{0_{\mu\nu}}(s_y) I_{0_{\mu\nu}}(s_z), \tag{3}$$

where

$$I^{g_x}_{0_{\mu,\nu}}(s_x) \equiv I^{g_x}_{0_{\alpha,\beta}}(s_x) = \int_{-\infty}^{+\infty} (x - x_A)^n \, e^{-\alpha(x-x_A)^2} (x - x_B - g_x)^m \, e^{-\beta(x-x_B-g_x)^2} \, e^{-is_x x} \, dx, \quad (4)$$

α and β are the exponents of the GTFs associated with AO $\mu(A)$ and $\nu(B)$.

$I^{g_x}_{0_{\alpha,\beta}}(s_x)$ will be referred to as the static scattering integral and is calculated analytically with the method proposed by Ferrero [6]. In this last expression, the reference system $\mathscr{R} \equiv (O, x, y, z)$ is chosen for the quantum calculation of the wave function, and n, m are the degrees of the x polynomial that depend on the nature of the AOs encountered (s, p, d, etc.).

Introduction of thermal motion

In order to calculate the structure factors $F_T(\boldsymbol{s})$ at any temperature T, it is necessary to know the mean square displacements $\langle u^2 \rangle$ of the atoms in the cell. The values of $\langle u^2 \rangle$ are either experimental, in most cases determined from neutron scattering studies, or are obtained from an optimization between experimental and theoretical structure factors.

In the context of the Debye hypothesis, the probability $p(\boldsymbol{u}_A)$ of finding atom A with a displacement $\boldsymbol{u}_A$ with respect to its equilibrium position $\boldsymbol{r}_A$ follows the distribution law [7]:

$$p(\boldsymbol{u}_A) = \left[\frac{\det(\boldsymbol{B}_A^{-1})}{(2\pi)^3} \right]^{1/2} e^{-(1/2)\boldsymbol{u}_A^{\mathrm{T}} \boldsymbol{B}_A^{-1} \boldsymbol{u}_A}, \quad (5)$$

where $\boldsymbol{B}_A$ is the tensor of mean square displacements, of which each element is written as

$$\boldsymbol{B}_{A,ij} = \langle u_{A,i} u_{A,j} \rangle \quad i, j \equiv x, y, z. \quad (6)$$

The values of $\boldsymbol{B}_A$ are given in the crystallographic system $(O, \boldsymbol{a}_1, \boldsymbol{a}_2, \boldsymbol{a}_3)$ and so they must be transformed to the working system $\mathscr{R}$.

Crystallographers usually take thermal motion into account by, first dividing the total electron density into atomic contributions $\rho_A(\boldsymbol{r})$ leading to atomic scattering factors $f_{0,A}$, and then correcting them by the Debye–Waller exponential term. In this model of independent atoms, the structure factor is written as

$$F_T^{\mathrm{DW}}(\boldsymbol{s}) = \sum_A f_{0,A}(\boldsymbol{s}) \, e^{-(1/2)\boldsymbol{s}^{\mathrm{T}} \boldsymbol{B}_A \boldsymbol{s}} \, e^{-i\boldsymbol{s}\cdot\boldsymbol{r}_A} \quad (7)$$

In the present work, we are proposing another way of calculating the structure factor at temperature T $F_T(\boldsymbol{s})$ that introduces in the mean value of the operator $e^{-i\boldsymbol{s}\cdot\boldsymbol{r}}$ the atomic displacements $\boldsymbol{u}$ distributed with probability functions $p(\boldsymbol{u})$. Our method is based on the assumption that the AOs follow the movements of the associated atoms, and that the corresponding elements of the density matrix $\boldsymbol{P}^{\boldsymbol{g}}_{\mu\nu}$ are, on a statistical average point of view, unchanged at the different temperatures.

In the Debye hypothesis, where atoms are in mutually independent vibration, the variables u_A and u_B are separated. In addition, when the thermal agitation tensors $\boldsymbol{B}_A$ and $\boldsymbol{B}_B$ are simultaneously diagonal, which is very often the case, the expression $F_T(\boldsymbol{s})$ becomes easier to calculate because the coordinates $u_{A,x}, \ldots, u_{B,x}, \ldots$ can also be separated. In this case, $F_T(\boldsymbol{s})$ becomes formally identical to (3):

$$F_T(\boldsymbol{s}) = \sum_{\alpha,\beta,\boldsymbol{g}} \boldsymbol{P}^{\boldsymbol{g}}_{\alpha,\beta} \, I^{g_x}_{T_{\alpha,\beta}}(s_x) I^{g_y}_{T_{\alpha,\beta}}(s_y) I^{g_z}_{T_{\alpha,\beta}}(s_z), \quad (8)$$

where the integral of dynamic scattering $I^{g_x}_{T_{\alpha,\beta}}(s_x)$ is the mean value of $I^{g_x}_{0_{\alpha,\beta}}(s_x)$(4) over the displacements $u_{A,x}$ and $u_{B,x}$:

$$I^{g_x}_{T_{\alpha,\beta}}(s_x) = \int_{-\infty}^{+\infty}\int_{-\infty}^{+\infty}\left\{\frac{1}{\sqrt{2\pi \boldsymbol{B}_{A,xx}}}\,\mathrm{e}^{-(1/2)(u^2_{A,x}/\boldsymbol{B}_{A,xx})}\,\frac{1}{\sqrt{2\pi \boldsymbol{B}_{B,xx}}}\,\mathrm{e}^{-(1/2)(u^2_{B,x}/\boldsymbol{B}_{B,xx})}\right\}$$
$$\times\left\{\int_{-\infty}^{+\infty}(x - x_A - u_{A,x})^n\,\mathrm{e}^{-\alpha(x-x_A-u_{A,x})^2}\,(x - x_B - g_x - u_{B,x})^m\right.$$
$$\left.\times\,\mathrm{e}^{-\beta(x-x_B-g_x-u_{B,x})^2}\,\mathrm{e}^{-\mathrm{i}s_x x}\,\mathrm{d}x\right\}\mathrm{d}u_{A,x}\,\mathrm{d}u_{B,x}. \tag{9}$$

The calculation of the integral (9) is shown in Appendix A. In the case of s or p orbitals ($n = 0, 1$; $m = 0, 1$), it leads to

$$I^{g_x}_{T_{\alpha,\beta}}(s_x) = \left(\frac{\alpha'_x}{\alpha}\right)^{n+1/2}\left(\frac{\beta'_x}{\beta}\right)^{m+1/2} I^{g_x}_{0_{\alpha'_x,\beta'_x}}(s_x), \tag{10}$$

where

$$\alpha'_x = \frac{\alpha}{1 + 2\alpha \boldsymbol{B}_{A,xx}} \quad \text{and} \quad \beta'_x = \frac{\beta}{1 + 2\beta \boldsymbol{B}_{B,xx}}. \tag{11}$$

It should be also noted that the exponents α'_x and β'_x defined by (11) are always less than the corresponding exponents α and β. This shows that the effect of thermal motion is to render GTFs more diffuse. When $T \to 0$ K, $\boldsymbol{B} \to 0$, then $\alpha'_x \to \alpha$, $\beta'_x \to \beta$ and we have the expression of the static scattering integral $\boldsymbol{I}^{g_x}_{0_{\alpha,\beta}}(s_x)$.

When the two orbitals are centered on the same atom A, integration involves only the displacement $\boldsymbol{u}_A$ of the atom, and in this case, regardless of the type of orbitals, we have an expression that includes the Debye–Waller term $\mathrm{e}^{-(1/2)\boldsymbol{B}_{A,xx}s_x^2}$:

$$\boldsymbol{I}^0_{T_{\alpha,\beta}}(s_x) = \boldsymbol{I}^0_{0_{\alpha,\beta}}(s_x)\,\mathrm{e}^{-(1/2)\boldsymbol{B}_{A,xx}s_x^2}. \tag{12}$$

These integrals $\boldsymbol{I}^{\boldsymbol{g}}_{T_{\alpha,\beta}}(\boldsymbol{s})$ and $\boldsymbol{I}^{\boldsymbol{0}}_{T_{\alpha,\beta}}(\boldsymbol{s})$ are the terms of a rectangular matrix $\boldsymbol{I}^{\boldsymbol{g}}_{T}(\boldsymbol{s})$ shown below in the simple case of two orbitals per cell, each described by a single Gaussian and centered on different atoms, A and B.

$$\boldsymbol{I}^{\boldsymbol{g}}_{T}(\boldsymbol{s}) = \begin{array}{c} \\ \textbf{cell 0} \\ \textbf{cell 1} \\ \\ \textbf{cell } \boldsymbol{g} \end{array} \begin{array}{c} \textbf{cell 0} \\ \left[\begin{array}{cc} \boldsymbol{I}^{\boldsymbol{0}}_{T_{\alpha,\alpha}} & \boldsymbol{I}^{\boldsymbol{0}}_{T_{\beta',\alpha'}} \\ \boldsymbol{I}^{\boldsymbol{0}}_{T_{\alpha',\beta'}} & \boldsymbol{I}^{\boldsymbol{0}}_{T_{\beta,\beta}} \end{array}\right. \\ \left[\begin{array}{cc} \boldsymbol{I}^{\boldsymbol{1}}_{T_{\alpha',\alpha'}} & \boldsymbol{I}^{\boldsymbol{1}}_{T_{\beta',\alpha'}} \\ \boldsymbol{I}^{\boldsymbol{1}}_{T_{\alpha',\beta'}} & \boldsymbol{I}^{\boldsymbol{1}}_{T_{\beta',\beta'}} \end{array}\right. \\ \vdots \\ \left.\begin{array}{cc} & \end{array}\right] \end{array}$$

It is well-known that, for $\boldsymbol{s} = \mathbf{0}$, the static structure factor must coincide with the total number of electrons enclosed in an elementary cell. At temperature T, this number is not exactly recovered with the present method. As we shall see in the following, this condition is nevertheless verified with a precision better than 0.1% which is still much smaller than the agreement factors between theoretical and experimental values.

3 Applications and results

Structure factors at 0 and 298 K were calculated with relationships (3) and (8), and compared to the most recent experimental values, reputed to be precise since they are corrected for systematic errors of absorption, dispersion and thermal diffuse scattering (TDS). The compounds chosen were silicon, magnesium oxide and beryllium oxide in order to present and discuss the results obtained with different crystal structures and different types of bonding. The calculated values $F_0(\boldsymbol{s})$ and $F_T(\boldsymbol{s})$ are listed in Tables 1 (Si), 2 (MgO) and 3 (BeO) of Appendix B and compared with experimental findings $[F_T(\text{ref.})]$ in Figs. 1 (Si), 2 (MgO) and 3 (BeO), where for each $h\,k\,l$ reflection the relative difference $[F_T^{(\text{calc.})} - F_T^{(\text{ref.})}]/F_T^{(\text{ref.})}$ is represented (symbol ◆).

As an indication, the importance of thermal correction for the structure factor was also evaluated using the relative difference $|F_T^{(\text{calc.})} - F_0^{(\text{calc.})}|/F_0^{(\text{calc.})}$ and represented on the same figures by the symbol ⊡.

Finally, the agreement factor

$$R = \frac{\sum_{h\,k\,l} |F_T^{(\text{calc.})} - F_T^{(\text{ref.})}|}{\sum_{h\,k\,l} F_T^{(\text{ref.})}}$$

was calculated for each compound in order to analyze the overall quality of agreement with experimental findings.

Silicon. Silicon has a face-centered cubic structure (diamond type). The only spots in a diffraction film are $h\,k\,l$ of the same parity. The symmetry of the structure and the occupation of high symmetry sites by silicon atoms explain the isotropic character of atomic thermal motion. The value $8\pi^2 \boldsymbol{B}_{\text{Si}} = 0.4632\ \text{Å}^2$, obtained by Spackman [8] from an optimization between calculated and experimental structure factors, was used in the present work.

The $F_T(\boldsymbol{s})$ values obtained with our method and those calculated with the Debye–Waller relationship (7), which is written in the case of silicon:

$$F_T^{\text{DW}}(\boldsymbol{s}) = F_0(\boldsymbol{s})\, \text{e}^{-8\pi^2 \boldsymbol{B}_{\text{Si}} ((\sin\theta)/\lambda)^2} \tag{13}$$

are listed in columns 4 and 5 of Table 1 for the 18 reflections explored by Spackman.

Several theoretical values of $F_0(\boldsymbol{s})$ were recently calculated by Pisani et al. [9] using different atomic orbital basis sets describing the Si atom. The $F_0(\boldsymbol{s})$ values adopted in Table 1 (column 3) were calculated with Eq. (3) using the richest AO basis set, 8-411G**.

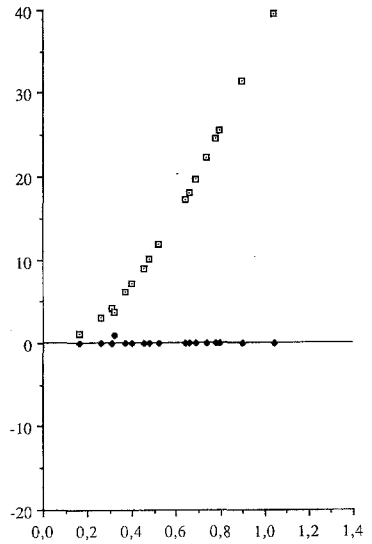

Fig. 1. *Silicon*: variations of the expressions $[F_T^{(\text{calc.})} - F_T^{(\text{ref.})}]/F_T^{(\text{ref.})}$ (◆) and $[F_T^{(\text{calc.})} - F_0^{(\text{calc.})}]/F_0^{(\text{calc.})}$ ([⊡]) versus $\sin\theta/\lambda$ corresponding to the different reflections $h\,k\,l$ (Table 1). $F_T^{(\text{calc.})}$ and $F_0^{(\text{calc.})}$ are the dynamic and static structure factors calculated with Eqs (8) and (3). $F_T^{(\text{ref.})}$ are the experimental values given by Spackman [8]

Furthermore, the reference values used in Fig. 1 and for the calculation of R are those obtained with relationship (13), where the static structure factors $F_0(\boldsymbol{s})$ correspond to the experimental values of Spackman [8].

Examination of Fig. 1 (symbol ◆) and the value $R = 0.2\%$ show that the agreement with experimental data is excellent.

Magnesium oxide. Magnesium oxide has a face-centered cubic structure (NaCl type). For the same reasons as in the case of silicon, the thermal motion of the Mg^{2+} and O^{2-} ions is isotropic and results in a diagonal tensor $\boldsymbol{B}$ with three identical components. The values adopted in the present work are

$$8\pi^2 \boldsymbol{B}_{Mg^{2+}} = 8\pi^2 \boldsymbol{B}_{O^{2-}} = 8\pi^2 \boldsymbol{B} = 0.336\ \text{Å}^2.$$

They were obtained from the optimization between theoretical structure factors calculated by Causà et al. [3] and experimental structure factors determined by Lawrence [10]. These data were preferred to those of Sanger [11] for the reasons discussed in [3].

Magnesium oxide is a fully ionic compound and so is treated with the model of independent atoms: the static structure factor of each species $F_{0,Mg^{2+}}$ and $F_{0,O^{2-}}$ is obtained by adding the electron density contributions in each energy band that are unambiguously attributable to either magnesium or to oxygen. In these conditions, the structure factor at T calculated with the Debye–Waller relationship (7) is

$$F_T^{\text{DW}}(\boldsymbol{s}) = [F_{0,Mg^{2+}}(\boldsymbol{s}) \pm F_{0,O^{2-}}(\boldsymbol{s})]\, e^{-8\pi^2 \boldsymbol{B}((\sin\theta)/\lambda)^2}, \tag{14}$$

where the + and − signs are used each time reflection in direction $\boldsymbol{s}$ corresponds to all odd $h\,k\,l$ and all even $h\,k\,l$, respectively.

The terms $F_{0,Mg^{2+}}(\boldsymbol{s})$ and $F_{0,O^{2-}}(\boldsymbol{s})$ in Eq. (14) were calculated in this work using the methodology of Causà et al. [3], but with the use of stricter calculation conditions, identical to those used for silicon [9], and an enriched AO basis set for Mg and O with d polarization functions on each atom [12]. The values thus obtained are listed in columns 3 and 4 of Table 2. In spite of these new conditions, a very slight variation of structure factors in small angle zones ($(\sin\theta)/\lambda \leqslant 0.5\ \text{Å}^{-1}$)

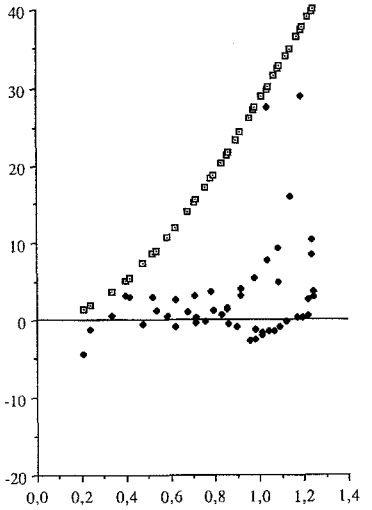

Fig. 2. *Magnesium oxide*: same legend as for Si in Fig. 1. $F_T^{(\text{ref.})}$ are the experimental values given by Sanger [11].

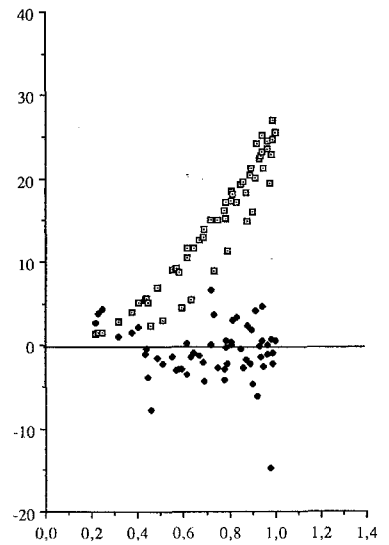

Fig. 3. *Beryllium oxide*: same legend as for Si in Fig. 1. $F_T^{(\text{ref.})}$ are the experimental values given by Vidal-Valat et al. [14].

is observed. The $F_T^{\text{DW}}(s)$ values (14) are listed in column 6 of Table 2 in order to compare them with the $F_T(s)$ values derived with Eq. (8).

In order to compare our theoretical results to the experimental data of Sanger [11], most numerous in small angle zones, the values in column 6 were corrected by taking into account the phenomenon of anomalous dispersion [11]. Figure 2 and the value of factor of agreement $R = 1.74\%$, show that agreement is satisfactory between our results and those of Sanger. It should be noted that five low intensity reflections, 751, 931, 933, 771 and 755 are responsible for a considerable difference that can reach 29%. When they are not included, the value of R becomes 1.52%.

Beryllium oxide. The choice of this compound is justified because it enables our calculations to be extended to a hexagonal compact, anisotropic crystal structure (wurtzite type) and to a partially covalent bond.

In a prior study [13] the structure factors $F_T^{DW}(\boldsymbol{s})$ were calculated with Eq. (7):

$$F_T^{DW}(\boldsymbol{s}) = F_0(\boldsymbol{s}) = e^{-8\pi^2 \bar{\boldsymbol{B}}((\sin\theta)/\lambda)^2} \tag{15}$$

adopting a mean square deviation $8\pi^2 \bar{\boldsymbol{B}} = 0.3063$ Å^2 defined by

$$\bar{\boldsymbol{B}} = \frac{m_{Be}\boldsymbol{B}_{Be} + m_O B_O}{m_{Be} + m_O}$$

and resulting from optimization between our values calculated with expression (15) and the experimental values of Vidal-Valat et al. [14]. The agreement factor $R = 3.7\%$ shows that the quality of agreement is moderate, partially explained by the large relative difference characterizing all reflections corresponding to $l = 4$.

Stricter calculation conditions defined in the study of silicon and the use of a richer atomic orbital basis set developed for the study of the elastic constants of BeO [15] were adopted in the present work. They furnish the values of $F_0(\boldsymbol{s})$ listed in columns 3 and 4 of Table 3 and calculated from the methodology adopted previously in the case of MgO.

The introduction of thermal motion requires the use of anisotropic $\boldsymbol{B}$ tensors, involving four parameters that must be separately optimized in order to obtain the best possible agreement with experimental findings. To avoid these numerous calculations, the values proposed by Vidal–Valat et al. [14] were used:

$$8\pi^2 \boldsymbol{B}_{Be,xx} = 8\pi^2 \boldsymbol{B}_{Be,yy} = 0.3237 \text{ Å}^2, \qquad 8\pi^2 \boldsymbol{B}_{Be,zz} = 0.4185 \text{ Å}^2,$$
$$8\pi^2 \boldsymbol{B}_{O,xx} = 8\pi^2 B_{O,yy} = 0.2763 \text{ Å}^2, \qquad 8\pi^2 B_{O,zz} = 0.2842 \text{ Å}^2$$

and the $F_T^{DW}(\boldsymbol{s})$ values thus deduced from Eq. (7) are listed in column 6 of Table 3.

Figure 3 and the new value of the overall factor of agreement $R = 2.3\%$ are a substantial improvement over prior results [13], also confirmed by the satisfying agreement of practically all $l = 4$ reflections. This improvement was brought about by including the anisotropic thermal motion tensors. These observations are confirmed by examining the curves showing the effect of thermal agitation (symbol ⊡), which clearly show the existence of two branches: the lower branch corresponds to the nine $l = 4$ reflections. This result confirms the necessity of treating thermal motion in BeO anisotropically.

4 Discussion and conclusion

In this work, we have calculated dynamic structure factors $F_T(\boldsymbol{s})$ including atomic vibrations resulting from thermal motion. We assume that the atomic orbitals follow the motion of the corresponding nuclei while the matrix density remains invariant. The normalization of $F_T(\boldsymbol{s} = \boldsymbol{0})$ is an essential point to our method. In the case of silicon (the most unfavourable case) $F_T(\boldsymbol{s} = \boldsymbol{0}) = 13.981$ which is within 0.1% of the exact value of 14.

Our method (expression (8) of $F_T(\boldsymbol{s})$) was compared with the classical Debye–Waller model (expression (7) of $F_T^{DW}(\boldsymbol{s})$) which is customally used by crystallographers to correct atomic scattering factors. The results obtained with either of these methods are very similar, practically at the limit of the calculation precision at large values of $\sin\theta/\lambda$.

This result is entirely consistent in the case of ionic compounds (MgO) since there is practically no orbital overlap and since the terms $I^0_{T_{\alpha,\beta}}(\boldsymbol{s})$ of relationship (12) correspond to the Debye–Waller correction.

In the case of the covalent crystal, silicon, with considerable orbital overlap, the general situation is as if all the matrix elements $I^g_T(\boldsymbol{s})$ were corrected in the same way by the Debye–Waller factor, but in the region of small values of $\sin\theta/\lambda$, which is the most affected by the valence electrons, the difference between $F_T(\boldsymbol{s})$ and $F^{\mathrm{DW}}_T(\boldsymbol{s})$ is more clearly pronounced. In particular, the difference between these two structure factors for the reflection (2 2 2), representing the asphericity of the electron distribution around the silicon atom, is much larger (1%). In addition, these calculations pertain to room temperature, i.e. to low values of mean square difference $\langle u^2\rangle$. The differences between $F_T(\boldsymbol{s})$ and $F^{\mathrm{DW}}_T(\boldsymbol{s})$ increase for $\boldsymbol{B}$ values one order of magnitude larger (amplitudes of atomic vibrations about three times higher). They lead to a deviation of 0.30% for the first three reflections and 10% for the reflection (2 2 2). This result shows clearly the influence of the orbital overlap on the calculated structure factors.

Finally, it is important to stress that our method $F_T(\boldsymbol{s})$ is easily implemented, and that the computation costs of the calculations is comparable to that of the static case. In our opinion, the main advantage is that this method does not require any prescription for subdividing the total density into atomic contributions, which may be rather artificial in some cases. Our calculation program relies on the matrix density $\boldsymbol{P}^g$ reproduced by the CRYSTAL program, since vibronic correction directly affects each atomic orbital in each cell g of the crystal. Thus this method requires no intermediate step, such as the projection of $\boldsymbol{P}^g$ on energy bands $E_n(\boldsymbol{k})$ that we have also carried out in the case of MgO and BeO for the calculations of dynamic structure factors in the Debye–Waller model.

Appendix A

Given to calculate Eq. (9) which can be also written as

$$
\begin{aligned}
I^{g_x}_{T_{\alpha,\beta}}(s_x) = \int_{-\infty}^{+\infty}\int_{-\infty}^{+\infty}\int_{-\infty}^{+\infty} & (x - x_A - u_{A,x})^n \, \mathrm{e}^{-\alpha(x-x_A)^2} \\
& \times (x - x_B - g_x - u_{B,x})^m \, \mathrm{e}^{-\beta(x-x_B-g_x)^2} \, \mathrm{e}^{-\mathrm{i}S_x x} \\
& \times \frac{1}{\sqrt{2\pi \boldsymbol{B}_{A,xx}}} \exp\left\{ -\left(\alpha + \frac{1}{2\boldsymbol{B}_{A,xx}}\right)\left[u_{A,x} - \frac{\alpha(x-x_A)}{\alpha + 1/2\boldsymbol{B}_{A,xx}}\right]^2 \right\} \\
& \times \exp\left\{ \left(\alpha + \frac{1}{2\boldsymbol{B}_{A,xx}}\right)\left[\frac{\alpha(x-x_A)}{\alpha + 1/2\boldsymbol{B}_{A,xx}}\right]^2 \right\} \\
& \times \frac{1}{\sqrt{2\pi \boldsymbol{B}_{B,xx}}} \exp\left\{ -\left(\beta + \frac{1}{2\boldsymbol{B}_{B,xx}}\right)\left[u_{B,x} - \frac{\beta(x-x_B-g_x)}{\beta + 1/2\boldsymbol{B}_{B,xx}}\right]^2 \right\} \\
& \times \exp\left\{ \left(\beta + \frac{1}{2\boldsymbol{B}_{B,xx}}\right)\left[\frac{\beta(x-x_B-g_x)}{\beta + 1/2\boldsymbol{B}_{B,xx}}\right]^2 \right\} \mathrm{d}u_{A,x}\, \mathrm{d}u_{B,x}\, \mathrm{d}x .
\end{aligned}
$$

The principal integral on x is not limited, but given the mathematical shape of the electron functions (Gaussian), x varies within a limited domain around the atom. As a result of this, the following variable changes can be carried out:

$$u'_{A,x} = u_{A,x} - \frac{\alpha(x - x_A)}{\alpha + 1/2\boldsymbol{B}_{A,xx}} \quad \text{and} \quad u'_{B,x} = u_{B,x} - \frac{\beta(x - x_B - g_x)}{\beta + 1/2\boldsymbol{B}_{B,xx}},$$

where x is considered to be a constant.

Using the new exponents

$$\frac{\alpha}{\alpha + 1/2\boldsymbol{B}_{A,xx}} = 2\boldsymbol{B}_{A,xx}\alpha'_x \quad \text{and} \quad \frac{\beta}{\beta + 1/2\boldsymbol{B}_{B,xx}} = 2\boldsymbol{B}_{B,xx}\beta'_x,$$

we obtain

$$\begin{aligned} I^{g_x}_{T_{\alpha,\beta}}(s_x) = \int_{-\infty}^{+\infty} & e^{-\alpha'_x(x - x_A)^2} e^{-\beta'_x(x - x_B - g_x)^2} e^{-iS_x x} \frac{1}{\sqrt{2\pi \boldsymbol{B}_{A,xx}}} \\ & \times \int_{-\infty}^{+\infty} [x - x_A - u'_{A,x} - 2\boldsymbol{B}_{A,xx}\alpha'_x(x - x_A)]^n e^{-\alpha u'^2_{A,x}/2\boldsymbol{B}_{A,xx}\alpha'_x} du'_{A,x} \\ & \times \frac{1}{\sqrt{2\pi \boldsymbol{B}_{B,xx}}} \int_{-\infty}^{+\infty} [x - x_B - g_x - u'_{B,x} - 2\boldsymbol{B}_{B,xx}\beta'_x(x - x_B - g_x)]^m \\ & \times e^{-\beta u'^2_{B,x}/2\boldsymbol{B}_{B,xx}\beta'_x} du'_{B,x}\, dx. \end{aligned} \tag{A1}$$

Now that the two displacement variables u'_A and u'_B are separated, we have to calculate the following integrals:

$$\int_{-\infty}^{+\infty} \left[\frac{\alpha'_x}{\alpha}(x - x_A) - u'_{A,x} \right]^n e^{-\alpha u'^2_{A,x}/2\boldsymbol{B}_{A,xx}\alpha'_x} du'_{A,x}.$$

There are three cases, depending on the type of orbitals involved, the most complicated being that of d_x2 for which $n = 2$.

$$\begin{aligned} & \int_{-\infty}^{+\infty} \left(\frac{\alpha'_x}{\alpha}\right)^2 (x - x_A)^2 e^{-\alpha u'^2_{A,x}/2\boldsymbol{B}_{A,xx}\alpha'_x} du'_{A,x} \\ & \quad - 2\frac{\alpha'_x}{\alpha}(x - x_A) \int_{-\infty}^{+\infty} u'_{A,x} e^{-\alpha u'^2_{A,x}/2\boldsymbol{B}_{A,xx}\alpha'_x} du'_{A,x} \\ & \quad + \int_{-\infty}^{+\infty} u'^2_{A,x} e^{-\alpha u'^2_{A,x}/2\boldsymbol{B}_{A,xx}\alpha'_x} du'_{A,x}. \end{aligned} \tag{A2}$$

The second integral is null since the function is odd in $u'_{A,x}$. Concerning the other two, a mathematical formula is used that involves hermitian functions:

$$\int_{-\infty}^{+\infty} w^{2l} e^{-\gamma w^2} dw = \frac{(2l - 1)!!}{2^l} \sqrt{\frac{\pi}{\gamma^{2l+1}}}.$$

We thus have for (A2):

$$\left[\left(\frac{\alpha'_x}{\alpha}\right)^2 (x - x_A)^2 + \boldsymbol{B}_{A,xx}\frac{\alpha'_x}{\alpha} \right] \sqrt{\pi \Big/ \frac{1}{2\boldsymbol{B}_{A,xx}} \frac{\alpha}{\alpha'_x}}$$

It is possible to include the three cases $n = 0, 1, 2$ in a single expression:

$$\left[\left(\frac{\alpha'_x}{\alpha}\right)^n (x - x_A)^n + \boldsymbol{B}_{A,xx}\frac{\alpha'_x}{\alpha}\delta(n-2)\right]\sqrt{2\boldsymbol{B}_{A,xx}\pi}\sqrt{\frac{\alpha'_x}{\alpha}}.$$

The first term in brackets is in fact always present, for $n = 0$ (in which case it is equal to 1) as well as for $n = 1$ or $n = 2$. Concerning the second term, it appears only for d_{x^2} orbitals when n is equal to 2, which is why we have added the Kronecker symbol $\delta(n-2)$. Adding these values to expression (A1), we obtain

$$\begin{aligned} I^{g_x}_{T_{\alpha,\beta}}(s_x) = \int_{-\infty}^{+\infty} & \mathrm{e}^{-\alpha'_x(x-x_A)^2}\,\mathrm{e}^{-\beta'_x(x-x_B-g_x)^2}\,\mathrm{e}^{-s_x x} \\ & \times\left(\frac{\alpha'_x}{\alpha}\right)^{n+1/2}\left[(x-x_A)^n + \boldsymbol{B}_{A,xx}\left(\frac{\alpha'_x}{\alpha}\right)^{1-n}\delta(n-2)\right] \\ & \times\left(\frac{\beta'_x}{\beta}\right)^{m+1/2}\left[(x-x_B-g_x)^m + \boldsymbol{B}_{B,xx}\right. \\ & \left.\times\left(\frac{\beta'_x}{\beta}\right)^{1-m}\delta(m-2)\right]\mathrm{d}x \end{aligned} \tag{A3}$$

We have static integrals with new exponents α'_x and β'_x: $I^{g_x}_{0\alpha'_x,\beta'_x}(s_x)$.

Appendix B

Table 1. Static $F_0(s)$ and dynamic $F_T(s)$, $F_T^{\mathrm{DW}}(s)$ structure factors of *silicon* calculated with Eqs. (3), (8) and (7), respectively.

hkl	$(\sin\theta)/\lambda$	$F_0(s)$	$F_T(s)$	$F_T^{\mathrm{DW}}(s)$
111	0.160	10.755	10.624	10.628
220	0.260	8.640	8.371	8.374
311	0.305	8.004	7.661	7.666
222	0.319	0.217	0.20902	0.20701
400	0.368	7.465	7.009	7.011
331	0.401	7.269	6.746	6.747
422	0.451	6.730	6.123	6.125
333	0.478	6.426	5.781	5.781
511	0.478	6.459	5.810	5.810
440	0.521	6.060	5.345	5.344
444	0.638	4.983	4.127	4.127
551	0.658	4.815	3.942	3.940
642	0.689	4.556	3.657	3.657
800	0.737	4.187	3.258	3.256
660	0.781	3.871	2.918	2.918
555	0.797	3.758	2.800	2.800
844	0.902	3.147	2.159	2.159
880	1.042	2.536	1.535	1.534

The computational procedure, the truncation conditions adopted for the calculated wavefunction, the atomic orbital basis set 8-411G** and the lattice parameter $a_0 = 5.431$ Å used in this study were already described by Pisani et al. [9].

Table 2. *Magnesium oxide*: same comment as for Si.

hkl	$(\sin\theta)/\lambda$	$F_{0,Mg}(s)$	$F_{0,O}(s)$	$F_T(s)$	$F_T^{DW}(s)$
111	0.205	8.669	5.935	10.779	10.779
200	0.237	8.292	5.246	53.141	53.140
220	0.336	7.018	3.632	41.018	41.015
311	0.393	6.263	2.967	12.521	12.518
222	0.411	6.042	2.881	33.727	33.724
400	0.475	5.281	2.466	28.734	28.731
331	0.517	4.814	2.176	9.649	9.646
420	0.531	4.675	2.191	24.990	24.987
224	0.581	4.187	2.006	22.116	22.114
115	0.616	3.882	1.848	7.160	7.159
333	0.616	3.882	1.846	7.170	7.166
440	0.671	3.462	1.777	18.015	18.013
531	0.702	3.253	1.677	5.343	5.341
600	0.712	3.189	1.701	16.503	16.501
442	0.712	3.189	1.702	16.505	16.503
620	0.750	2.961	1.642	15.239	15.238
533	0.778	2.813	1.573	4.049	4.048
226	0.787	2.768	1.592	14.166	14.165
444	0.822	2.604	1.551	13.244	13.243
711	0.847	2.496	1.501	3.130	3.129
551	0.847	2.496	1.500	3.132	3.131
640	0.855	2.463	1.514	12.441	12.440
642	0.888	2.342	1.481	11.736	11.735
731	0.911	2.262	1.442	2.481	2.480
553	0.911	2.262	1.442	2.482	2.481
800	0.949	2.146	1.424	10.550	10.549
733	0.971	2.084	1.393	2.017	2.016
820	0.978	2.065	1.398	10.045	10.045
644	0.978	2.065	1.398	10.046	10.045
228	1.007	1.995	1.374	9.588	9.587
660	1.007	1.995	1.374	9.588	9.587
751	1.027	1.947	1.348	1.682	1.681
555	1.027	1.947	1.348	1.683	1.682
662	1.034	1.932	1.351	9.170	9.169
840	1.061	1.877	1.329	8.785	8.784
911	1.081	1.839	1.307	1.438	1.438
753	1.081	1.839	1.307	1.439	1.438
842	1.087	1.827	1.308	8.430	8.429
664	1.113	1.783	1.287	8.101	8.100
931	1.132	1.752	1.268	1.260	1.260
844	1.162	1.706	1.248	7.506	7.505
933	1.180	1.681	1.231	1.129	1.128
771	1.180	1.681	1.231	1.129	1.128
755	1.180	1.681	1.231	1.129	1.128
1000	1.186	1.673	1.229	7.236	7.235
860	1.186	1.673	1.229	7.236	7.235
1020	1.210	1.643	1.211	6.981	6.981
862	1.210	1.643	1.211	6.981	6.981
951	1.227	1.622	1.195	1.030	1.029
773	1.227	1.622	1.195	1.030	1.030
1022	1.233	1.615	1.193	6.741	6.740
666	1.233	1.615	1.193	6.741	6.741

The computational procedure and truncation conditions are the same as those described for Si. The AO basis set is given in [12] and the lattice parameter is $a_0 = 4.215$ Å.

Table 3. *Beryllium oxide*: same comment as for Si.

hkl	$(\sin\theta)/\lambda$	$F_{0,\mathrm{Be}}(s)$	$F_{0,\mathrm{O}}(s)$	$F_T(s)$	$F_T^{\mathrm{DW}}(s)$
100	0.216	0.924	2.973	7.689	7.691
002	0.230	1.829	5.509	11.598	11.599
101	0.244	1.566	4.453	6.933	6.930
102	0.315	0.848	1.979	4.237	4.237
110	0.374	1.595	3.216	9.235	9.237
103	0.407	1.328	2.506	6.714	6.716
200	0.431	0.744	1.325	3.915	3.917
112	0.439	1.474	2.646	5.777	5.778
201	0.446	1.264	2.264	3.075	3.074
004	0.460	1.435	2.526	2.148	2.147
202	0.489	0.690	1.159	2.527	2.529
104	0.508	0.672	1.130	0.896	0.896
203	0.552	1.092	1.796	4.839	4.841
210	0.571	0.614	1.012	2.955	2.955
211	0.582	1.045	1.703	2.197	2.196
114	0.592	1.188	1.933	1.434	1.433
105	0.614	0.995	1.636	4.382	4.383
212	0.615	0.573	0.940	2.000	2.000
204	0.630	0.560	0.914	0.673	0.673
300	0.647	1.091	1.810	5.130	5.131
213	0.667	0.916	1.529	3.937	3.938
302	0.687	1.024	1.721	3.542	3.543
006	0.690	1.019	1.716	3.302	3.303
205	0.719	0.842	1.454	3.675	3.676
106	0.723	0.483	0.831	1.572	1.572
214	0.733	0.475	0.818	0.630	0.629
220	0.747	0.927	1.641	4.359	4.359
310	0.778	0.440	0.799	2.076	2.076
222	0.782	0.874	1.583	3.077	3.077
116	0.784	0.870	1.579	2.881	2.881
311	0.786	0.752	1.358	1.655	1.655
304	0.794	0.857	1.555	1.245	1.244
215	0.810	0.722	1.350	3.192	3.194
312	0.811	0.416	0.774	1.475	1.475
206	0.813	0.414	0.772	1.385	1.385
107	0.833	0.694	1.314	1.715	1.715
313	0.851	0.673	1.312	2.963	2.964
400	0.863	0.381	0.754	1.825	1.826
401	0.870	0.650	1.280	1.527	1.527
224	0.877	0.742	1.468	1.241	1.240
402	0.893	0.361	0.734	1.320	1.320
216	0.895	0.360	0.732	1.242	1.243
314	0.903	0.355	0.722	0.619	0.618
207	0.913	0.604	1.248	1.584	1.584
008	0.920	0.689	1.454	3.248	3.250
403	0.929	0.587	1.248	2.640	2.641
320	0.940	0.333	0.718	1.624	1.625
108	0.944	0.330	0.716	1.565	1.566
306	0.946	0.659	1.418	2.327	2.328
321	0.947	0.569	1.221	1.429	1.429
315	0.967	0.550	1.221	2.531	2.532
222	0.968	0.317	0.701	1.193	1.193
404	0.978	0.311	0.691	0.613	0.612
217	0.986	0.531	1.194	1.475	1.475
410	0.988	0.611	1.395	3.020	3.020
118	0.993	0.607	1.391	2.913	2.915
323	1.001	0.517	1.195	2.375	2.375

The computational procedure and truncation conditions are the same as those described for Si. The AO basis set is given in [13, 15] and the lattice parameters are: $a_0 = 2.677$ Å; $c_0 = 4.350$ Å; $u_0 = 0.3774$.

Acknowledgement. The authors wish to express their gratitude to Prof. Pisani for his helpful suggestions and discussions.

References

1. Dovesi R, Pisani C, Roetti C, Causá M, Saunders VR (1988) Crystal 88 QCPE, Program n°577, Indiana University Bloomington Indiana
2. Pisani C, Dovesi R, Roetti C (1988) Hartree Fock ab initio treatment of crystalline systems, Springer, Berlin, Heidelberg, New York
3. Causá M, Dovesi R, Pisani C, Roetti C (1986) Acta Cryst B42:247
4. Cohen-Tannoudji C, Dupont-Roc J, Grynberg G (1988) In: Processus d'Interaction entre Photons et Atomes, CNRS
5. Azavant P (1994) Approche théorique de la diffusion élastique et inélastique dans les solids par la méthode ab initio Hartree–Fock: Application aux sulfines de lithium et de sodium, Thesis, University of Pau
6. Ferrero E (1981) Studio Hartree–Fock della struttura elettronica di sistemi metallici: applicazione al litio, Thesis, University of Torino
7. Willis BTM, Pryor AW (1975) In: Thermal vibrations in crystallography, ch 4, p 96, Cambridge
8. Spackman MA (1986) Acta Cryst A42:271
9. Pisani C, Dovesi R, Orlando R (1992) Int J Quantum Chem 42:5
10. Lawrence JL (1973) Acta Cryst A29:94
11. Sanger PL (1969) Acta Cryst A25:694
12. Dovesi R, Roetti C, Freyria-Fava C, Aprá E, Saunders VR, Harrison VR (1992) Phil Trans R Soc London A341:203
13. Lichanot A, Chaillet M, Larrieu C, Dovesi R, Pisani C (1992) Chem Phys 164:383
14. Vidal-Valat G, Vidal JP, Kurki-Suonio K, Kurki-Suonio R (1987) Acta Cryst A43:540
15. Lichanot A, Rerat M (1993) Chem Phys Lett 211:249